IMPACT OF VIBRATION ON TILLAGE PERFORMANCE OF SUBSOILERS USING THE DISCRETE ELEMENT METHOD (DEM)

/

振动对深松机耕作性能影响的离散元法研究

Shi Zhiming, Chen Tonghao, Li Shoutai, Yang Ling, Yang Mingjin*) [1]

Southwest University, College of Engineering and Technology, Chongqing Key Laboratory of Agricultural Equipment for Hilly and Mountainous Regions / P. R. China

**Correspondence: Tel: +86-13883002509; E-mail: ymingjin@swu.edu.cn*

DOI: https://doi.org/10.35633/inmateh-64-08

Keywords: *subsoiling, vibration, tillage performance, DEM, field experiment*

ABSTRACT

Plow pan is one of the main obstacles to high production of agricultural plants in Chongqing, China. As a minimal tilling method, subsoiling can break the plow pan and help the growth of agricultural plants. There are two subsoiling methods: vibrating subsoiling (VS) and traditional subsoiling (TS). A soil model with upland field features in Chongqing was established for DEM-based simulation. The simulation was validated by field experiments, in items of soil looseness, coefficient of soil disturbance, and cross-section of tillage, the errors of the simulated and experimental values of the soil looseness and soil disturbance coefficient of TS and VS were 12.9% and 14.7%, respectively. Compared with TS, VS resulted in lower soil looseness, higher coefficient of soil disturbance, smaller width of upper furrow, and lighter damage of tillage layer, and no obvious overturn of soil blocks was observed for the VS. Compared with TS, vibration helps improve the tillage performance of subsoilers.

摘要

犁底层是中国重庆地区农业高产的主要障碍之一。作为一种少耕方法，深松可以打破犁底层，并有助于农业作物生长。有两种深松法：振动深松法和传统深松法。用离散元法建立了重庆地区田间土壤模型。通过田间试验，在土壤膨松度，土壤扰动系数和耕作横截面方面对仿真结果进行了验证，TS 和VS 后的土壤膨松度和土壤扰动系数的仿真值和实验值的误差分别为12.9%和14.7%。与传统深松相比，振动深松降低了土壤膨松度，增加了土壤扰动系数，减小了上部沟形宽度，对土壤耕作层破坏较小，地表无明显翻土。与传统深松相比，振动有助于提高深松机的耕作性能。

INTRODUCTION

Small handheld tillers are universally employed in Chongqing, China. More than 99.5% of power tillers are of small handheld tillers in Chongqing since riding power tillers are unsuitable for tilling operation in the small hilly farmlands. Plow pan with thickness of 5-10 cm was formed by long term tillage of small handheld tillers, and it was one of the main obstacles to high production of agricultural plants (*Ma C. et al, 2017; Geroy I.J. et al, 2011*). Subsoiling, as a minimal tilling method (*Sun J.Y. et al, 2018*), can break the plow pan, improve the soil structure, and then help the growth of agricultural plants (*Hang C.G. et al, 2017*).

Vibration, electroosmosis and bionic method are main approaches to reducing traction resistance in subsoiling (*Sun J.Y. et al, 2018*). According to whether vibration occurs during operation, subsoiling was divided into vibrating subsoiling (VS) and traditional subsoiling (TS). The latter was a non-vibrating subsoiling method (*Liu X.H. et al, 2014*). As for VS, a periodic vibration was applied to the subsoiler in the vertical direction, and the vibration affected traction resistance, power consumption and tillage performance (*Niyamapa T. et al, 2010*).

While considering the soil disturbance, how to choose the subsoiling method is a problem that needs attention. However, the present research focuses on the drag reduction effect of VS, the influence of different vibrating sources, and subsoiling machine structure and other factors on subsoiling effect.

[1] *ZM Shi, Ms.; TH Chen, Ms.; ST Li, Ms.; L Yang, Prof.; MJ Yang, Prof.*

Few comprehensive simulation and experiment methods were used to comprehensively analyze the impact of VS and TS on soil disturbance behavior, soil furrow shape.

At present, most of the researches on soil subsoiling were carried out by using direct measurement method of field experiment or soil bin experiment and finite element method simulation. The direct measurement method was limited by factors such as weather, time, manpower and material resources. The finite element method was mainly for continuous media, and the soil could only be studied as a whole object. While the soil belongs to a discontinuous medium, the finite element method could not accurately analyze the interaction between subsoiler and soil particles, and it could not analyze the movement of soil particles after subsoiling to evaluate the soil subsoiling effect (*Mouazen A.M. et al, 1999*). Discrete element method (DEM), as a general method to study the discontinuous medium, could well solve the deficiencies of finite element method in the study of soil subsoiling (*Kasisira L.L. et al, 2006*).

The arc-shaped subsoiler had excellent farming performance compared with the linear shape under the condition of small length-to-depth ratio due to its convenient production and strong crushing ability. Therefore, the arc-shaped subsoiler was selected as the experiment machine in this study. According to the physicochemical properties of cultivated soil and the requirements of subsoiling operation in Chongqing hilly and mountainous area, the soil model was established based on the DEM, and the effects of VS and TS on soil disturbance behavior, soil furrow profile were analyzed.

MATERIALS AND METHODS

Move model

Subsoiler move

VS tilled the soil under the joint action of the vibrating element and the soil resistance. The periodic reciprocating vibrating element transmitted the force to the shank to drive the tine. The vibrating soil cutting was realized at locations of tine face and tine edge.

Compared with TS, the VS had one more periodic motion in the vertical direction. The equation of motion of vibrating subsoiler was simplified as:

$$x = v \cdot t \text{ , [mm]} \quad (1)$$

$$y = A \cdot \sin \omega t \text{ , [mm]} \quad (2)$$

where:

v is the horizontal movement speed, [mm/s];

t is the time, [s];

A is the amplitude, [mm];

ω is the angular velocity, [rad/s].

Soil move

The traditional subsoiler could be regarded as rigid, and it completes soil cutting, crushing, lifting and other actions at the same time under the drive of traction power (*Li X. et al, 2012*). The subsoiler moved forward, and the soil was periodically fractured along the shear surface under the cutting edge of the subsoiler, then the soil was partially lifted due to the mutual squeezing action (*Guo Z.J. et al, 2001*). The forces acting on the soil at this time included the frictional force, shearing force, squeezing force and the cutting force of the tine edge. The sum of the horizontal components of these forces was the resistance received by subsoiler during the tillage process (*Li B. et al, 2018*). The cutting process of traditional subsoiler in the soil was simplified to a low-speed moving inclined surface in the soil. The basic feature of this effect was that the soil repeatedly fails due to shearing, and the soil was repeatedly compressed to form many small soil blocks (*Momozu M. et al, 2002*), as shown in Fig. 1a.

In the case of VS, the subsoiler changed from one-dimensional cutting to two-dimensional vibration cutting. The original single motion process of the subsoiler was divided into two different stages: shearing the soil and lifting the soil (*Shmulevich, I., 2010*). After the subsoiler entered the soil, it rotated due to soil resistance and compresses the elastic element. The elastic element accumulated energy. After the soil reached the yield limit, the soil was broken, and the elastic element released energy to make the subsoiler rotate to complete the shearing process. After the soil was broken, the elastic element further released energy to make the subsoiler complete the lifting of the soil. At this time, the force of the soil on the subsoiler was almost perpendicular to the direction of traction, so the resistance was greatly reduced, as shown in Fig. 1b.

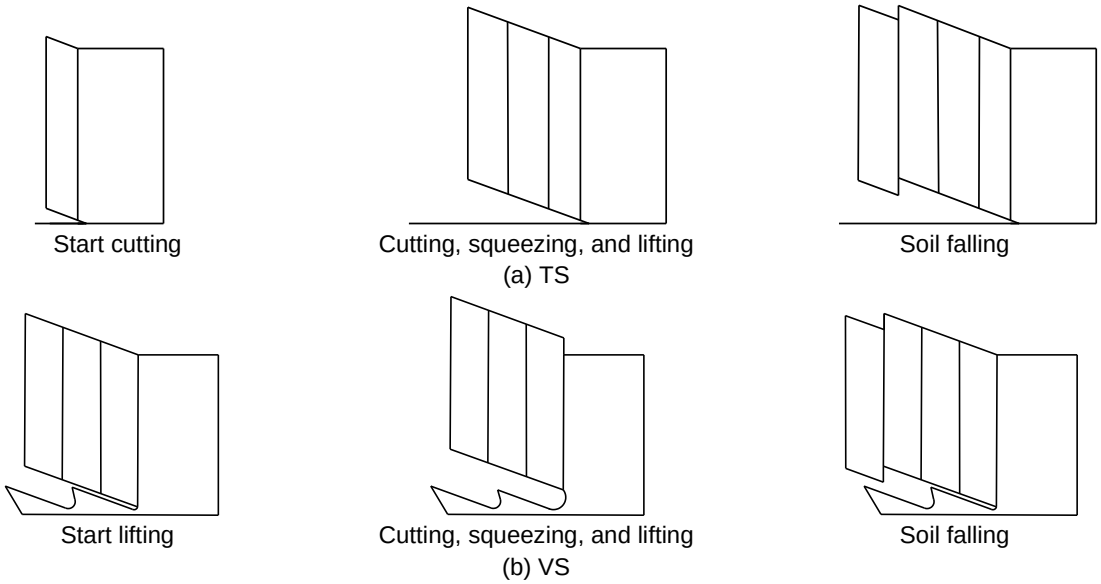

Fig. 1 - Soil move under TS and VS

Subsoiling simulation

Experiment method

In this study, DEM was used for simulation experiments, combined with the soil quality and physicochemical properties of the hilly and mountainous areas of Chongqing. A soil bin model was established in the software of EDEM (Engineering Discrete Element Method), and the geometric model of the subsoiler created was imported. After completion, the simulation experiment was started, and the results were exported and analyzed.

Subsoiler model

According to the Chinese standard (JB/T9788-1999), an arc-shaped subsoiler was selected for the experiment, and the subsoiler consisted of an arc-shaped shank and a chisel-shaped tine, as shown in Fig. 2. The subsoiler installation height H was 680mm, the straight shank height H_1 was 320mm, the shank width b was 60mm, the tine length L was 165mm, the arc-shaped shank radius R was 303mm, and the tine blade angle α was 20°.

In order to ensure the accuracy of the simulation, the three-dimensional structural model of the subsoiler for simulation was established by using software of Creo3.0 with ratio of 1:1 and saved it in igs. format.

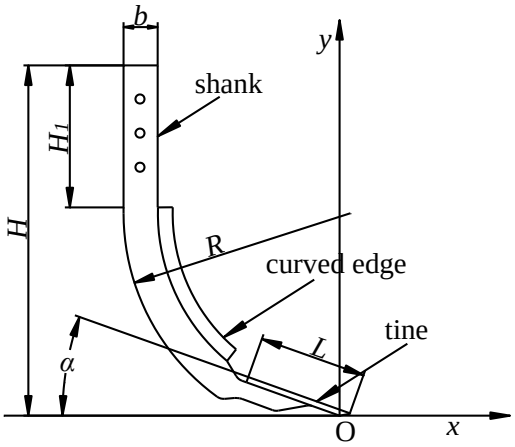

Fig. 2 - Schematic diagram of subsoiler

Soil particle and soil contact model

In order to make EDEM simulation experiments reliable, it was necessary to create a more accurate virtual soil model. Soil particles were mainly composed of lump, nuclei, and column (Yang, Q. et al, 2019). Using the self-contained particles (3mm in diameter) in the EDEM as the basic structural unit, models of lump, nuclear and columnar soil particle were obtained (*Tadesse, D., 2010*), as shown in Fig. 3.

Considering the type of purplish soil in the hilly and mountainous regions of Chongqing, the Hertz-Mindlin with Bonding model in EDEM was used to create a contact model between soil particles.

This model made the particles had bond like the actual soil hydraulic bridge force in the field (as shown in Fig. 3e), which could withstand a certain amount of force and torque (*Wang Y., 2014*).

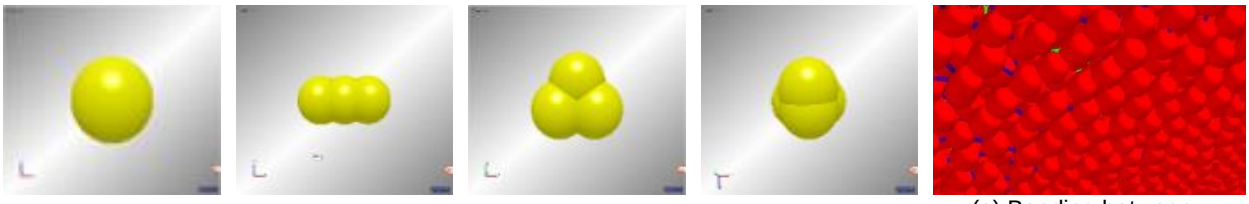

(a) Lump 1 (b) Column (c) Nuclei (d) Lump 2 (e) Bonding between particles

Fig. 3 - Model of soil particles and their bonding model

Soil model parameters

The main parameters of the selected soil contact model included the coefficient of restitution, the dynamic and static friction coefficients of soil to soil and soil to subsoiler. The parameters were mainly from data in the references (*Wang Y., 2014; Ucgul M. et al, 2014*).

The main parameters of the soil bin model were listed in Table 1.

Table 1

Main parameters of soil bin model

Parameter	Value	Parameter	Value
Soil bin dimensions (length, width, height) [mm]	1000×1200×400	Coefficient of static friction of soil-soil	0.55
Subsoiler speed [mm/s]	830	Coefficient of restitution of soil-65Mn steel	0.35
Tillage depth [mm]	250	Coefficient of rolling friction of soil-65Mn steel	0.09
Soil particle density [kg/m^3]	1920	Coefficient of static friction of soil-65Mn steel	0.55
Poisson's ratio of soil	0.4	Radius of the filling element [mm]	3
Shear modulus of soil [Pa]	1×10^7	Number of soil particles	680000
Density of 65Mn steel [kg/m^3]	7830	Acceleration of gravity [m/s^2]	9.81
Poisson's ratio of 65Mn steel	0.35	Simulation time [s]	10
Shear modulus of 65Mn steel [Pa]	7.27×10^{10}	Amplitude [mm]	20
Coefficient of restitution of soil-soil	0.3	Frequency [Hz]	4
Coefficient of rolling friction of soil-soil	0.35	Angular velocity [rad/s]	8π

EDEM modeling

In order to ensure the simulation in consistency with the field experiment, according to the depth and width of the subsoiling, a soil bin model with dimensions of 1000 mm × 1200 mm × 400 mm (length × width × height) was created in EDEM, as shown in Fig. 4.

After the simulation parameter setting was completed, the soil particles were dynamically generated by the particle factory in the EDEM, and then the particles were settled and bonded to form a bond between the particles. In real soil particles, the size of soil particles of different types was not the same.

In order to make the soil bin model closer to the real soil, the size of soil particles generated was in normal distribution (*Wang, Y. 2014*).

Then import the 3D model of the subsoiler into the EDEM, set motion parameters of the subsoiler and the tillage depth to 250mm. After the simulation was completed, the data of TS and VS were saved.

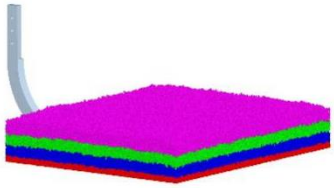

Fig. 4 - EDEM simulation soil model

Field experiment

Experiment site and materials

The experiment site located at the experimental field next to the engineering training center of Southwest University, with length of 15 m and width of 6.5 m. The soil in the experimental field was purplish soil.

Experimental process

Before the experiment, the experimental field was simply treated, the soil debris such as grass roots and stones were removed, and leveling treatment was carried out. The measurement of the basic parameters of the soil in the experimental field was completed according to the experiment requirements. The average of the measurement results is shown in Table 2.

Table 2

Soil parameters of experiment field

Parameter	Density [kg/m^3]	Moisture content [%]	Firmness [Pa]
Value	1920	36.5	642700

After the soil parameter measurement was completed, the TS and VS were experimented in turn. The traction power was from a riding type tractor (Dongfanghong LX2004, China). According to requirements of subsoiling of farming soil in Chongqing, the moving speed of subsoiler was selected as 830 mm/s with the tillage depth 250mm. After tilling operation, a self-made simple soil cross-sectional profile measuring instrument was used to measure the soil data of different subsoiler. In order to ensure the accuracy of the measurement results, the soil data under the action of each subsoiler were measured in three different positions with an interval of 1.0m, and the soil data were recorded, as shown in Fig. 5.

(a) TS

(b) VS

(c) Measurement after subsoiling

Fig. 5 - Scenery of field experiment

RESULTS

Comparative analysis of soil disturbance

In order to study the impact of TS and VS on the soil disturbance behavior of different soil layers, the longitudinal sections at tilling time 0.05 s, 0.25 s, 0.45 s, 0.65 s, and 0.85 s were selected and plotted, as shown in Fig. 6. The effects of subsoiling on the overall soil disturbance were obtained as well, as shown in Fig. 7. Compared with TS, VS had one more vertical motion of sine vibration, and its vibration parameters were listed in Table 1.

As seen from Figs. 6 and 7, different subsoiling mechanisms of VS and TS were observed. Firstly, for TS, the subsoiler moved forward under the action of traction. The tine and the curved cutting edge of the subsoiler successively contacted the plow pan in the soil.

The cutting and squeezing of the plow pan made it rise and break down at the same time, which disturbed the cultivated layer (magenta particles in Fig. 6) and formed a certain ridge on the surface. As the subsoiling progressed, the ridge formed on the ground broke and failed under the shearing action of the shank, and finally backfilled into the subsoiling soil pit under the gravity. Secondly, for VS, the subsoiling process was divided into two different stages: shearing and lifting the soil. The subsoiler moved forward under the action of traction. The tine and the curved edge of the subsoiler contacted successively the plow pan in the soil. The shearing and squeezing of the plow pan caused it to break and fail. Due to the presence of vibration, the plow pan was sheared, squeezed, and lifted. With the tilling of the soil, the shear plane periodically sheared and lifted, which formed a periodic intermittent shear plane. Compared with TS, VS had a larger disturbance range on the soil particles of the plow pan, and the effect of loosening soil was strengthened.

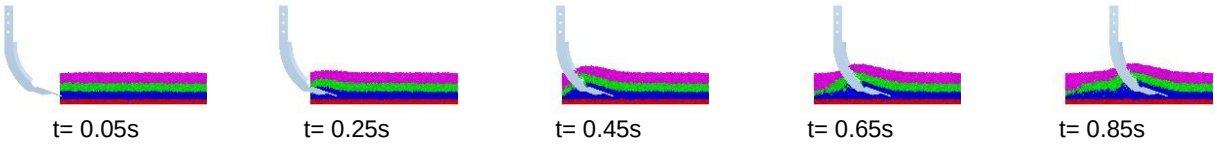

(a) TS at different time points

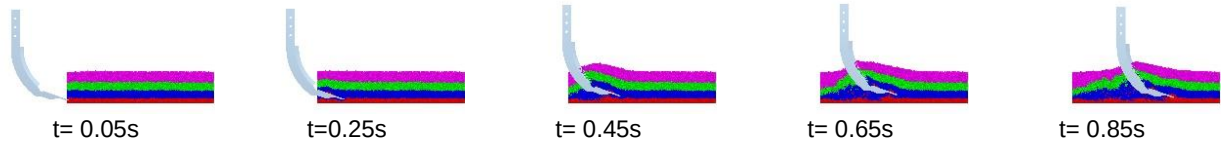

(b) VS at different time points

Fig. 6 - The effects of subsoiling on the vertical disturbance of each layer of soil

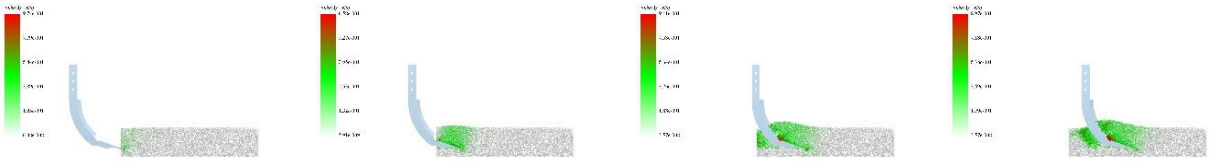

(a) TS at different time points

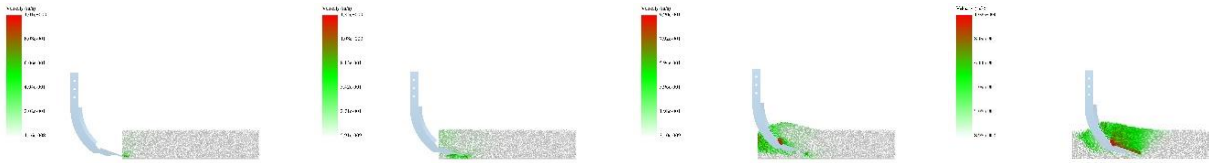

(b) VS at different time points

Fig. 7 - The effects of subsoiling on the overall soil disturbance range

Analysis of soil disturbance effect

The soil looseness and soil disturbance coefficient were commonly used to evaluate the disturbance effect of soil (*Hang, C. G. et al, 2017*). The effect of soil disturbance after subsoiling was shown in Fig. 8. The soil looseness and soil disturbance coefficient were expressed as:

$$\rho = \frac{A_h - A_q}{A_q} \times 100\% \text{ , [\%]} \tag{3}$$

$$y = \frac{A_s}{A_q} \times 100\% \text{ , [\%]} \tag{4}$$

where:

ρ is the soil looseness, [%];

A_h is the cross-sectional area formed by the post-tillage soil surface and the boundary of the standard furrow described in Chinese Standards for Subsoiling Implements (JB/T10295-2014), [mm^2];

A_q is the cross-sectional area formed by the un-tilled soil surface and the boundary of the standard furrow, [mm²]; y is the soil disturbance coefficient, [%];

A_s is the cross-section area formed by the un-tilled soil surface and the actual furrow from field experiment, [mm²].

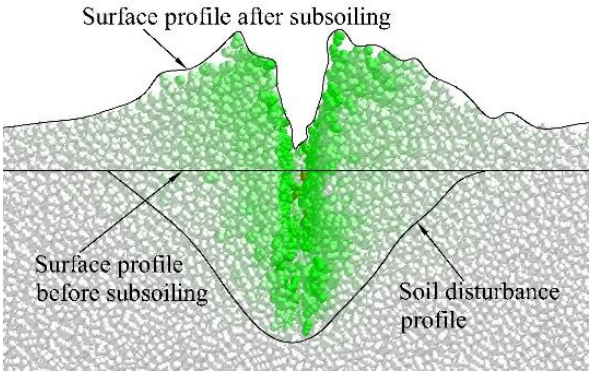

Fig. 8 - Effect diagram of soil disturbance

The profile of soil disturbance after subsoiling was shown in Fig.9. According to provisions of the Chinese standard (GB/T 24675.2-2009) "Conservation Tillage Machine-Subsoiler", the quality evaluation of subsoiling should meet requirements: operation was soil looseness within range of 10%-40%, and soil disturbance coefficient larger than 50%. The simulation and experiment values and relative errors of soil looseness and soil disturbance coefficient after TS and VS were calculated from equations (3) and (4), as listed in Table. 3.

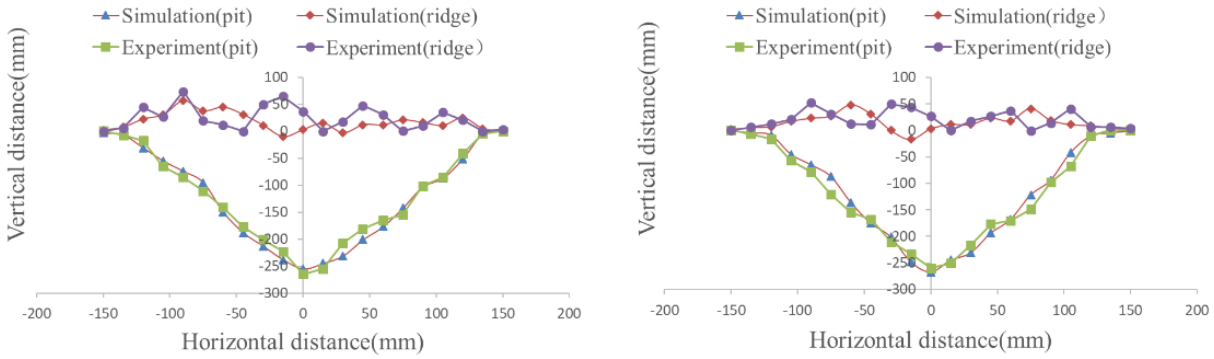

(a) TS (b) VS

Fig. 9 - Effect of subsoiling on soil disturbance profile

Table 3

Simulation and experiment results of soil looseness and disturbance coefficient

Subsoiling method	Soil looseness			Soil disturbance coefficient		
	Simulation value [%]	Experiment value [%]	Relative error [%]	Simulation value [%]	Experiment value [%]	Relative error [%]
TS	27.1	24.4	11.1	62.1	54.2	14.6
VS	26.5	23.3	13.7	65.3	56.5	15.6

As seen from Table 3, the soil disturbance after VS and TS met requirements of provisions of the Chinese standard. Compared with TS, VS had a smaller soil looseness and a larger soil disturbance coefficient. In addition, the mean errors of the simulated and experimental values of the soil looseness and soil disturbance coefficient of TS and VS were 12.9% and 14.7%, respectively. Then, the simulation model in this study could reveal the disturbance behavior of soil during the actual subsoiling process with good agreements.

The effect of subsoiling on furrow profile

The experiment and simulation results of the furrow profile after TS and VS were calculated and summarized, as listed in Table 4. The furrows of simulation and experiment were shown in Fig. 10. As seen from Table 4, TS and VS had significant influence on the V-shaped soil furrow. Compared with TS, the width of the upper furrow profile after the VS was obviously smaller, but there was no significant difference in the width of the lower furrow profile. As seen from Fig. 11, compared with TS, VS had less damage to the cultivated soil layer, and there was no significant overturning of the soil surface, which was beneficial to improve the soil's ability to store water and maintain moisture, and helpful for increase of crop yield.

Table 4

Width of furrow after subsoiling

Subsoiling method	Upper furrow width		Lower furrow width	
	Simulation value [mm]	Experiment value [mm]	Simulation value [mm]	Experiment value [mm]
TS	245	293	64	71
VS	213	247	61	75

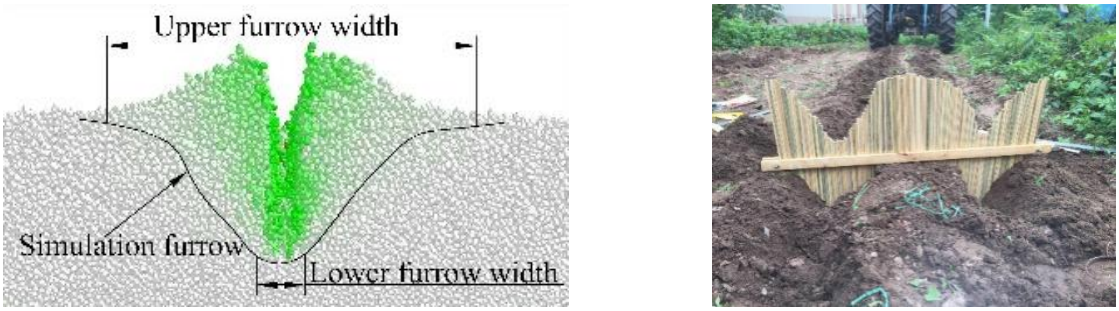

(a) Simulation furrow (b) Field experiment furrow

Fig. 10 - Furrow measurement after subsoiling

(a) Surface after TS (b) Surface after VS

Fig. 11 - Soil surface after subsoiling

CONCLUSIONS

Based on soil type in Chongqing, China, a soil model was established using EDEM and combined with field experiments. The effects of TS and VS on soil disturbance behavior, furrow profile were studied and analyzed. Main conclusions were drawn as follows:

(1) The DEM can accurately simulate the disturbance in the process of soil subsoiling, with good consistence with field experiment. The errors of the simulated and experimental values of the soil looseness and soil disturbance coefficient of TS and VS were 12.9% and 14.7%, respectively. Compared with TS, the soil of VS had less soil looseness and larger soil disturbance coefficient.

(2) TS and VS had a great impact on the furrow profile. Compared with TS, the width of the upper furrow profile of VS was obviously smaller, VS had less damage to the cultivated soil layer, and there is no obvious overturning of soil and lump on the surface. There was no significant difference in the width of the lower furrow profile between TS and VS.

ACKNOWLEDGEMENTS

The study was funded by Fundamental Research Funds for Central Universities, China (No.XDJK2018AC001) and Chongqing Science & Technology Commission (No. CSTC2016SHMSZX80037).

REFERENCES

[1] Geroy, I. J., Gribb, M. M., Marshall, H. P., Chandler, D. G., Benner, S. G. (2011). Aspect influences on soil water retention and storage. *Hydrological Processes*, Vol.25, Issue 25, pp.3836-3842, Ed. Southwest University; http://dx.doi.org/10.1002/hyp.8281.

[2] Guo, Z. J., Tong, J., Zhou, Z. L., Ren, L. Q. (2001). Status and prospect of subsoiler technology research (深松技术研究现状与展望). *Transactions of the Chinese Society of Agricultural Engineering*, Vol.17, Issue 6, pp.169-174, Ed. Chinese Society of Agricultural Engineering, Beijing/P.R.C.

[3] Hang, C. G., Huang, Y. X., Zhu, R. X. (2017). Analysis of the movement behavior of soil between subsoilers based on the discrete element method. *Journal of Terramechanics*, Vol.74, Issue 12, pp.35-43, Ed. Elsevier Sci Ltd, Oxford/England. https://doi.org/10.1016/j.jterra.2017.10.002.

[4] Kasisira, L. L., Plessis, H. L. M. D. (2006). Energy optimization for subsoilers in tandem in a sandy clay loam soil. *Soil & Tillage Research*, Vol.86, Issue 2, pp.185-198, Ed. Elsevier Sci Ltd, Oxford/England. https://doi.org/10.1016/j.still.2005.02.031.

[5] Liu, X. H., Yu, Y., Qiu, L. C. (2014). Design and experimental study on the vibration subsoiler. *Applied Mechanics & Materials*, Vol.707, Issue 12, pp.356-359, Ed. Helen Zhang, M. Han and X.J. Zhao. https://doi.org/10.4028/www.scientific.net/AMM.707.356.

[6] Li, X., Fu, J., Zhang, D., Cui, T., Zhang, R. (2012). Experiment analysis on traction resistance of vibration subsoiler (基于振动减阻原理的深松机牵引阻力试验). *Transactions of the Chinese Society of Agricultural Engineering*, Vol.28, Issue 1, pp.32-36, Ed. Chinese Society of Agricultural Engineering, Beijing/P.R.C.

[7] Li, B., Chen, Y., Chen, J. (2018). Comparison of two subsoiler designs using the discrete element method (DEM). *Transactions of the Asabe*, Vol.61, Issue 5, pp.1529-1537, Ed. American Society of Agricultural and Biological Engineers. DOI:10.13031/trans.12629.

[8] Ma, C., Meng, H., Kan, Z., Qi, J., (2017), The research current situation and development countermeasure of the orchard organic fertilizer deep application of disc ditching machine. *Journal of Agricultural Mechanization Research*, Vol.39, Issue 10, pp.12-17, 28.

[9] Mouazen, A. M. (1999). Finite element analysis of subsoiler cutting in non-homogeneous sandy loam soil. *Soil & Tillage Research*, Vol.51, Issue 1-2, pp.1-15, Ed. Elsevier Sci Ltd, Oxford/England. https://doi.org/10.1016/S0167-1987(99)00015-X.

[10] Momozu, M., Oida, A., Yamazaki, M., Koolen, A. J. (2002). Simulation of a soil loosening process by means of the modified distinct element method. *Journal of Terramechanics*, Vol.39, Issue 4, pp.207-220, Ed. Elsevier Sci Ltd, Oxford/England. https://doi.org/10.1016/S0022-4898(03)00011-9.

[11] Niyamapa, T., Namikawa, K. (2010). Force mechanics and soil disturbance of vibrating tillage tool. *Journal of Terramechanics*, Vol.37, Issue 3, pp.151-166, Ed. Elsevier Sci Ltd, Oxford/England. https://doi.org/10.1016/S0022-4898(00)00005-7.

[12] Sun, J. Y., Wang, Y. M., Ma, Y. H., Tong, J., Zhang, Z. J. (2018). DEM simulation of bionic subsoilers (tillage depth >40 cm) with drag reduction and lower soil disturbance characteristics. *Advances in Engineering Software*, Vol.119, Issue 5, pp.30-37, Ed. Elsevier Sci Ltd, Oxford/England. https://doi.org/10.1016/j.advengsoft.2018.02.001.

[13] Shmulevich, I. (2010). State of the art modeling of soil–tillage interaction using discrete element method. *Soil & Tillage Research*, Vol.111, Issue 1, pp.41-53, Ed. Elsevier Sci Ltd, Oxford/England. https://doi.org/10.1016/j.still.2010.08.003.

[14] Tadesse, D. (2010). Modelling soil structure, soil strength and material properties in DEM. *Advanced Engineering Materials*, Vol.13, Issue 1-2, pp.57-63, Ed. National Academic Research and Collaborations Information System. http://dx.doi.org/10.1002/adem.201000169.

[15] Ucgul, M., Fielke, J. M., Saunders, C. (2014). Three-dimensional discrete element modelling of tillage: determination of a suitable contact model and parameters for a cohesionless soil. *Biosystems Engineering*, Vol.121, Issue 5, pp.105-117, Ed. Elsevier Sci Ltd, Oxford/England. https://doi.org/10.1016/j.biosystemseng.2014.02.005.

[16] Wang, Y. Simulation analysis of structure and effect of the subsoiler based on DEM (基于离散元法的深松铲结构与松土效果研究), Master thesis of Jilin Agriculture University. 2014.

[17] Yang Q., Li, Z., Li H., He J., Wang Q., Lu C., (2019), Numerical Analysis of Particle Motion in Pneumatic Centralized Fertilizer Distribution Device Based on CFD-DEM. *Transactions of the Chinese Society for Agricultural Machinery*, Vol.50, Issue 8, pp.81-89, Ed. Chinese Society of Agricultural Engineering, Beijing/P.R.C.